Published in final edited form as:

Cancer Res. 2019 May 15; 79(10): 2736–2747. doi:10.1158/0008-5472.CAN-18-3872.

Melanoma-induced reprogramming of Schwann cell signaling aids tumor growth

Galina V. Shurin[1,a], **Oleg Kruglov**[2,a], **Fei Ding**[3], **Yan Lin**[3], **Xingxing Hao**[2], **Anton A. Keskinov**[1], **Zhaoyang You**[2,3,4], **Anna E. Lokshin**[3,5], **William A. LaFramboise**[1,3], **Louis D. Falo Jr.**[2,3,4], **Michael R. Shurin**[1,3,4], and **Yuri L. Bunimovich**[2,3,*]

[1]Department of Pathology, University of Pittsburgh Medical Center, Pittsburgh, PA, USA

[2]Department of Dermatology, University of Pittsburgh Medical Center, Pittsburgh, PA, USA

[3]Hillman Cancer Institute, University of Pittsburgh Medical Center, Pittsburgh, PA, USA

[4]Department of Immunology, University of Pittsburgh Medical Center, Pittsburgh, PA, USA

[5]Department of Medicine, University of Pittsburgh Medical Center, Pittsburgh, PA, USA

Abstract

The tumor microenvironment has been compared to a non-healing wound involving a complex interaction between multiple cell types. Schwann cells, the key regulators of peripheral nerve repair, have recently been shown to directly affect non-neural wound healing. Their role in cancer progression, however, has been largely limited to neuropathic pain and perineural invasion. In this study, we showed that melanoma activated otherwise dormant functions of Schwann cells aimed at nerve regeneration and wound healing. Such reprogramming of Schwann cells into repair-like cells occurred during the destruction and displacement of neurons as the tumor expanded and via direct signaling from melanoma cells to Schwann cells, resulting in activation of the nerve injury response. Melanoma-activated Schwann cells significantly altered the microenvironment through their modulation of the immune system and the extracellular matrix in a way that promoted melanoma growth in vitro and in vivo. Local inhibition of Schwann cell activity following cutaneous sensory nerve transection in melanoma orthotopic models significantly decreased the rate of tumor growth. Tumor-associated Schwann cells, therefore, can have a significant pro-tumorigenic effect and may present a novel target for cancer therapy.

Keywords

Melanoma; Schwann cell; nerve repair; tumor microenvironment

*Correspondence to: Yuri L. Bunimovich, MD, PhD, Department of Dermatology, University of Pittsburgh Medical Center, E1157 Thomas E. Starzl Biomedical Science Tower, 200 Lothrop Street, Pittsburgh, PA, 15213, bunimovichyl@upmc.edu.

[a]GVS and OK contributed equally to this work

Conflict of interest: The authors declare no conflict of interest.

INTRODUCTION

The peripheral nervous system (PNS) recently emerged as an important element of the tumor microenvironment, and has been implicated in the progression of several types of solid tumors, including prostate cancer, gastric cancer, basal cell carcinoma and pancreatic ductal adenocarcinoma.[1–4] The complexity of the PNS comprising motor, sensory and autonomic branches, and the challenges in studying these individual components resulted in a wide range of explanations of how the PNS may enhance the development or progression of cancer. The majority of reports on the interactions between solid malignancies and the PNS describe highly innervated cancers, where the presence of the nerve fibers within the tumor parenchyma may lead to cancer-related pain and malignant cell invasion as well as spread along the nerves, termed perineural invasion (PNI).[5–7] Primary cutaneous melanoma is not generally associated with pain, and PNI is not a usual critical mode of melanoma spread or a significant prognostic marker.[8, 9] We have determined here, however, that the intrinsic regenerative capacity of the PNS[10] is an important factor in melanoma growth.

While the number of investigations into the neuronal regulation of cancer has increased in recent years, the involvement of the peripheral neuroglia in cancer progression remains poorly understood.[11, 12] Schwann cells (SC) comprise the majority of the neuroglia of the PNS and are intimately associated with the nerve fibers, providing trophic support and a signaling scaffold for the axon.[13, 14] The investigations of SC in the context of cancer have been primarily focused on their important capability to promote neuropathic pain and PNI.[15, 16] However, until now the intrinsic role of SC in nerve regeneration has never been implicated in cancer progression.

Peripheral nerve repair occurs through a well described set of steps orchestrated by SC.[17, 18] After the nerve injury, such as crush or transection, SC lose the connection with the segment of the nerve distal to the insult, which regresses through a process called Wallerian degeneration. Accompanied by the large-scale change in their gene expression, both myelinated and non-myelinated SC distal to the nerve injury trans-differentiate into so-called repair-SC (rSC) capable of assisting with nerve regeneration through myelin debris clearing, local immune modulation, extracellular matrix remodeling and axon guidance.[10] Recently, similar activation of the peripheral glia was described in the context of cutaneous wound healing, where rSC disseminate from the injured nerves into the granulation tissue and support non-neural tissue repair.[19, 20]

The main goal of this study was to prove that melanoma-activated SC are functionally similar to neurotrauma-associated rSC, and that both types of SC can support tumor growth *in vivo*. We found that the selective nerve injury accelerates the growth of melanoma as a result of the modulation of the local microenvironment by activated rSC. Our results indicate that melanoma cells can directly reprogram SC into cells bearing high phenotypic and functional resemblance to rSC. We also found that primary human melanoma can induce nerve injury response and localized activation of SC in the tissue adjacent to the tumor. Importantly, blocking SC activity significantly decreases melanoma growth rate. Our results suggest that the plasticity of SC intended to assist with nerve repair is utilized by melanoma

to help create conditions favorable to tumor growth and progression. Therefore, Schwann cells represent an unexplored novel target for cancer therapy.

MATERIALS AND METHODS

Animals

C57BL/6 mice were purchased from Taconic Biosciences and The Jackson Laboratory. The inducible $Braf^{V600E}$/Pten-driven melanoma model (BP) was a gift from M. Bosenberg (Yale University, CT).[21] $Braf^{V600E}$/Pten-driven melanoma was generated by inducing oncogene $Braf^{V600E}$ expression with 4-hydroxytamoxifen (4-HT) (Sigma) in B6-$Tyr:Cre^{(ER)T2}Braf^{CA}Pten^{lox/lox}$ mice with correct genotype (presence of $Tyr:Cre^{(ER)T2}$, $Braf^{CA}$ and homozygous $Pten^{lox/lox}$).[22] Mice (7- to 8-week-old) were housed in a pathogen-free facility under controlled temperature, humidity, and 12-hour light/dark cycle with a commercial rodent diet and water available ad libitum. All studies were conducted in accordance with the NIH guidelines for the Care and Use of Laboratory Animals and approved by the Institutional Animal Care and Use Committee of the University of Pittsburgh (Pittsburgh, PA).

Cell lines

Primary human Schwann cells (SC) isolated from spinal nerve and primary mouse SC isolated from postnatal day 8 C57BL/6 sciatic nerve were purchased from ScienCell and cultured according to the manufacturer's protocols. B16 murine melanoma, RAW264.7 murine macrophages and human THP1 monocytes were purchased from ATCC. Human melanoma cell lines 397-mel, 526-mel and 624-mel were a gift from W. J. Storkus (University of Pittsburgh, PA). Mouse *Tyr::Cre(ER)T2; BRaf^{CA}; Pten$^{lox/lox}$* derived melanoma cell line (BPCL) was a gift from J. Wargo (MD Anderson Cancer Center, TX) and W. J. Storkus.[23] All primary and cell lines were authenticated, Mycoplasma tested, were contaminant free and used at low passage. Human melanoma and THP1 cell lines were cultured in RPMI-1640 medium supplemented with 2 mM of L-glutamine, 100 U/ml of penicillin, 100 μg/ml of streptomycin, 0.25 μg/ml amphotericin B (Sigma), 10 mM HEPES (Lonza), 55 μM 2-Mercaptoethanol (Gibco) and 10% heat-inactivated fetal bovine serum (FBS, Atlanta Biological). B16, BPCL and RAW264.7 cells were cultured in DMEM medium supplemented with 4 mM of L-glutamine, 100 U/ml of penicillin, 100 μg/ml of streptomycin, 0.25 μg/ml amphotericin B and 10% FBS. Human and murine primary SC were cultured in Schwann cell medium (SCM, ScienCell) supplemented with 1% (v/v) Schwann cell growth supplement, 1% (v/v) penicillin/streptomycin solution and 5% FBS (ScienCell).

Fluorescence microscopy

Collected tissue was fixed with 2% paraformaldehyde for 2 h and treated with 30% sucrose for 2 h. Specimens were frozen in 2-methyl butane (Sigma), then liquid nitrogen, and processed into 50 μm thick sections. Immunostaining was performed with primary antibodies at room temperature (RT) for 1 h, followed by FITC- or Cy5-labelled secondary antibodies and 4′,6-diamidino-2-phenylindole (DAPI) stain (Sigma). Sections mounted in gelvatol medium (Sigma) were imaged using Nikon A1+ confocal microscope at the Center

for Biological Imaging (University of Pittsburgh, PA). Image acquisition, processing and intensity analysis were performed with NIS-Elements AR 4.40 software (Nikon).

Collagen breakdown assay

Plates were coated with collagen I (Corning) film at 50 μg/cm^2 as described.[24] SC (2.5 × 10^4 cells) in 25 μl medium were placed on collagen film, covering approximately 20 mm^2 area, and incubated for 5 h at 37°C, 5% CO_2. After cell adhesion, SCM containing 20% (v/v) of: RPMI-1640 (human cells) or DMEM (mouse cells), or melanoma-conditioned medium with or without 40 μM minocycline was added to cover the entire collagen film. Cells were incubated for additional 96 h, followed by gentle trypsin removal. The intensity of light transmitted through collagen film was measured using ImageJ software. Values were normalized to the internal control intensity measured 10 mm away from the cells.

Mouse transplantable tumor model

C57BL/6 mice were injected intradermally with: (i) B16 cells (1×10^5 cells), (ii) B16 cells (1×10^5 cells) together with SC (1×10^5 cells), (iii) B16 cells (1×10^5 cells) with SC ((1×10^5 cells) pretreated in culture for 48 h with 40 μM minocycline and then washed, (iv) SC alone (1×10^5 cells), or (v) SC (1×10^5 cells) pretreated for 48 h prior to injection with 20% (v/v) of B16-conditioned medium. Tumor area (mm^2) was measured with a caliper.

Nerve transection procedure

Surgery: Cutaneous denervation was adapted from previously described technique.[25] Briefly, mice were anesthetized with isoflurane and approximately 1.5 cm skin incision was made along the midline back skin. Five dorsal cutaneous sensory nerves were transected approximately 5 mm lateral to the spinal cord. Skin was sutured with 7.0 prolene. Sham surgery included skin incision without nerve transection. After recovery, sensory denervation was confirmed with pin prick test.

Transplantable melanoma model: Nerve transection was performed on 8-week-old C57BL/6 mice. Next day, B16 melanoma cells (10^5 cells in 100 μl sterile PBS) were injected intradermally into the dorsolateral skin supplied by the cut nerves. Intradermal minocycline injections for appropriate groups (10 μM in 100μl PBS) were performed twice on the day before the surgery and once on the day of the surgery, in the same location on the back as melanoma injection.

Inducible melanoma model: 10 μl of 4-HT (Sigma) stock (10 mg in 200 μl of DMSO) was diluted in 30 μl of 100% ethanol and kept on ice. Braf^{V600E} expression in 8-week-old B6-Tyr-Cre^{ERT2}Braf^{CA}Pten$^{lox/lox}$ mice was induced by applying 2 μl of 4-HT on shaved skin of lateral back. Mice were immobilized until 4-HT dried completely. Transection of the sensory nerves supplying the dermatome of the induced melanoma was performed one week later. For appropriate groups, minocycline was injected (10 μM in 100μl PBS) daily for one week immediately after the surgery at the site of 4-HT application. Sham surgery (skin incision without nerve transection) was used as a control. Tumor area (mm^2) was measured as above.

Statistical Analysis

Results are expressed as mean ± SEM. Two-group analyses were performed using unpaired t test. Three or more groups with one independent variable were analyzed using one-way ANOVA with Tukey's multiple comparisons test. Three or more groups with two independent variables were analyzed using two-way ANOVA with Tukey's multiple comparisons test. Analyses were performed using GraphPad Prism software. All tests were two-tailed and a P value < 0.05 was considered to indicate statistical significance. Microarray and RNA sequencing data available in GEO database under accession numbers GSE126040 and GSE126076, respectively.

RESULTS

Neuroregulatory and neurodegenerative pathways are altered in melanoma

At an early stage of primary cutaneous melanoma invasion into the dermis malignant cells encounter a highly innervated tissue comprised of a dense network of myelinated and non-myelinated sensory and autonomic fibers of the PNS.[26] Since the innervation of melanoma is poorly characterized, we first examined primary cutaneous human melanoma for the presence of nerve fibers within the tumor and the surrounding tissue. Immunofluorescence analysis with antibodies against axonal and SC (both myelin- and nonmyelin-forming) markers, including PGP9.5, $p75^{NTR}$, GFAP, GAP43, KIF1A, S100β, MBP and MAG, revealed a significant reduction of the neuronal fibers and SC throughout majority of the tumor mass (Fig. 1A, B; Supplementary Fig. S1A, B). However, nerves and SC were detected in the tissue adjacent to the melanoma tumor (labeled *adjacent to tumor*). In contrast to the melanoma, the melanocytic nests of human nevi demonstrated intact innervation (Supplementary Fig. S1C). Interestingly, nerve fibers immunostained for GAP43 and $p75^{NTR}$, neuroplasticity markers of regenerating neurons and activated SC, respectively, were significantly more abundant in the tissue adjacent to the tumor, compared with tumor mass, nevus or normal skin (Fig. 1A–C; Supplementary Fig. S1C). There was no difference detected, however, between numbers of $PGP9.5^{+}$ fibers in the tissue adjacent to the tumor versus normal skin (Fig. 1A, B; Supplementary Fig. S1B, C). Neurons adjacent to the tumor often terminated before entering the tumor, and denervated SC, those which lost contact with the axon, were detectable in the tissue adjacent to the tumor (Supplementary Fig. S1D). These results suggest that during melanoma growth the intradermal nerve fibers are destroyed or displaced, resulting in the induction of nerve injury response and the activation of SC at the tumor edges.

To further elucidate the fate of the nerves during melanoma growth, we analyzed gene expression by RNA-sequencing in the patient-derived microdissected tissue collected from inside melanoma (labelled *tumor center*), comparing the results with the tissue adjacent to the tumor. To minimize the sampling error, three separate areas of the tumor were analyzed (Fig. 1D). In the tissue adjacent to the tumor, we detected 69 nerve and glia associated genes which were expressed at significantly higher levels compared to the tumor center (Supplementary Table S1). These genes function in neuronal structure and adhesion, axonal transport, myelin synthesis, axon guidance, neurite outgrowth, nerve migration, synapse, action potential, as well as neurotrophic factor and neuropeptide signaling. Importantly, a

number of these genes, including CHL1, GAL, GMFG, NGFR, NTN1, PTN and RELN participate in neuroregeneration and are known to be upregulated after nerve injury.[27, 28] Twenty-two genes closely associated with the nervous system were significantly overexpressed in the tumor center compared with the tissue adjacent to the tumor (Supplementary Table S1). Twenty of these genes, however, are known to be expressed at high levels by human melanoma cells (Supplementary Table S1).[29] Thus, the expression pattern of the neuronal/glial genes in the human melanoma tissue confirms the pathway toward exclusion of the nerve fibers from the tumor and further suggests the presence of the nerve injury response within the stroma adjacent to the tumor.

Pathway enrichment analysis of the gene expression data described above revealed common neuronal tissue related processes within the tumor center and the tissue adjacent to the tumor, including neurogenesis, wound healing (GO:0042060) and the extracellular matrix organization (GO:0030198) (Fig. 1E; Supplementary Table S1). Epidermis development (GO:0008544) and melanogenesis (hsa04916, GO:0042470) pathways were significantly overrepresented in the tissue adjacent to the tumor and tumor center, respectively, serving as confirmation that tissue microdissection accurately captured these domains (Fig. 1E; Supplementary Table S1). Enriched pathways unique to the tissue adjacent to the tumor included axon guidance (hsa04360, GO:0007411) and immune response (GO:0006955), while the melanoma center was uniquely enriched for neurodegeneration, neuron apoptotic process (GO:0051402), and positive regulation of neuron death (GO:1901216) (Fig. 1E; Supplementary Table S1). Taken together, the melanoma gene expression pattern and our observation that, at least in some cases, melanoma exhibits diminished innervation led us to hypothesize that in the process of expansion, melanoma may destroy or displace and damage the neuron projections and activate neurodegeneration mechanisms at the invading edge of the tumor.

Melanoma-induced phenotypic and functional changes of SC resemble SC activation during Wallerian degeneration

To test the hypothesis that melanoma can cause PNS neurodegeneration, we next determined whether human melanoma cell lines (397-mel, 526-mel, 624-mel) are able to convert human SC into activated cells resembling injury-induced repair SC. Nerve and tissue injury triggers trans-differentiation of SC into an immature phenotype of rSC.[10] This reprogramming is accompanied by well described changes in SC expression of specific key transcription factors and the downregulation of the genes of myelination. DNA microarray analysis of SC cultured in melanoma-conditioned medium revealed an enhancement of wound healing (GO: 0042060) and extracellular matrix reorganization (GO:0031012) functionalities (Supplementary Fig. S2 and Table S2). Furthermore, melanoma-activated SC (cultured in melanoma-conditioned medium or co-cultured with melanoma cells) shifted their gene expression profile to a more immature phenotype, highly resembling that of rSC. This was reflected in the upregulated expression of the markers of immature rSC, such as Id2, Egr1, c-Jun and Sox2, and the downregulation of the genes which drive terminal differentiation and myelination of SC, including Sox10, Egr2 and Oct6 (Fig. 2A, Supplementary Fig. S3A). In addition, the melanoma-dependent trans-differentiation of SC *in vitro* was accompanied by an activation of Erk and Akt signaling pathways, which are critical for the survival,

migration and repair activities of SC after the nerve injury (Fig. 2B, C).[30] Taken together, these results reveal phenotypic similarities between the nerve injury associated rSC and SC stimulated by melanoma cells.

We further examined whether melanoma-activated SC exhibit known functional attributes of rSC. During peripheral nerve repair, SC migrate, reorganize the extracellular matrix (ECM) and attract macrophages.[20] Recruited macrophages are polarized to a non-inflammatory M2 phenotype by the injured nerves and participate in the clearing of the myelin debris and wound healing.[31, 32] We determined that, similarly to rSC, melanoma-activated SC break down collagen matrix more readily compared to control SC (Fig. 3A; Supplementary Fig. S3B) and increase the production of factors (MMP1, FGF2, VEGF, IL6, MIF, AREG, BDNF, GDNF, Galectin 3, TGFβ1) which are critical to nerve/tissue repair, ECM reorganization, immune modulation, chemotaxis and myelin phagocytosis (Fig. 3B). Furthermore, melanoma-conditioned medium significantly enhanced SC motility (Fig. 3C; Supplementary Fig. S3C), as well as their ability to attract and polarize macrophages to the M2 type (Fig. 3D, E; Supplementary Fig. S3D). Consistent with these *in vitro* results, we found that the nerves at the invading edge of the primary human melanoma colocalize with the $CD68^{+}CD206^{+}$ M2-type macrophages, further suggesting the presence of the nerve injury-associated rSC-like cells within the tissue surrounding the melanoma (Fig. 3F). Taken together, our results demonstrate that melanoma can directly trans-differentiate SC into repair-like SC, activating their intrinsic functionality required for wound healing and nerve regeneration. Next, we hypothesized that the above-mentioned activities of repair-like SC in the melanoma microenvironment may promote tumor growth.

The repair phenotype and functionality of SC is also activated by murine melanoma cells

Before investigating the effect of activated SC on melanoma growth *in vivo*, we tested whether B16 and the inducible $BRAF^{V600E}/PTEN^{null}$ (BP) mouse melanoma cells have similar effects on mouse SC as those which human melanoma cells have on human SC. Intradermally injected B16 melanoma and inducible BP melanoma significantly increased the expression of ATF3, a marker of injured and regenerating neurons,[33] in the T10-L2 DRG of the sensory nerves supplying the melanoma compared with the DRG contralateral to the melanoma (Fig. 4A). This suggests that melanoma can activate the nerve injury response similarly to axotomy.[34] Furthermore, as the primary human melanoma, B16 and BP melanoma tumors showed an almost complete absence of axons and SC in the tumor center and increased intensities of markers of neuroplasticity and activated SC (GAP43, $p75^{NTR}$) in the tissue adjacent to melanoma compared with the control mouse skin (Fig. 4B–D). In line with our data on human melanoma, these results suggest that murine melanoma may also injure peripheral nerves during tumor growth and activate repair response in SC adjacent to the tumor.

To confirm and expand on our results with human SC, we examined whether mouse melanoma cells provoke a nerve injury response in SC *in vitro*. Supporting our *in vivo* data and consistent with above findings in human SC, mouse SC treated with conditioned medium of either BP melanoma derived cell line (BPCL)[23] or B16 melanoma cells suppressed the expression of the maturation and myelin genes (Egr2, periaxin, MBP, MPZ)

and upregulated the factors characteristic to the activated rSC (Olig1, c-Jun, GAP43, GDNF, $p75^{NTR}$, and PAX3) (Fig. 5A). As our human and murine data above showed that the phenotypic and functional changes of melanoma-activated SC closely resemble those of rSC associated with nerve injury, we next tested if minocycline could block melanoma's effect on SC. Minocycline was chosen because it inhibits the activity of rSC and slows the Wallerian degeneration and the nerve repair in rodent models of acute sciatic nerve injury. [35, 36] Consistent with these findings, we observed that mouse sciatic nerve explants treated *ex vivo* with minocycline immediately after nerve harvesting showed diminished MAPK/Erk signaling activation compared to the untreated controls, reflecting the reduced activation of SC exposed to minocycline (Fig. 5B). Minocycline also blocked the melanoma-dependent trans-differentiation from mature SC to repair-like SC *in vitro*: melanoma-stimulated SC treated with minocycline showed neither the expression pattern characteristic of rSC nor the activation of the MAPK/Erk signaling (Fig. 5A, C, D). However, in the absence of melanoma-conditioned medium, minocycline had no effect *in vitro* on SC expression of the above trans-differentiation markers (Supplementary Fig. S3E).

Just as we observed with human SC, mouse SC treated with B16- or BPCL-conditioned medium exhibited the characteristics of rSC, including enhanced motility and the ability to recruit macrophages and break down collagen (Fig. 5E–G; Supplementary Fig. S3F–H). These functions, characteristic of rSC, were blocked by treating melanoma-activated SC with minocycline, further illustrating that minocycline is an effective inhibitor of SC activation (Fig. 5E–G; Supplementary Fig. S3F–H). Taken together, these results show that murine melanoma-transdifferentiated SC, as human SC, are phenotypically and functionally similar to the nerve injury-associated rSC. Furthermore, SC reprogramming and activation triggered by either nerve transection or melanoma cells can be blocked with minocycline – a method we subsequently used to test the effect of activated SC on tumor growth *in vivo*.

Melanoma or nerve transection-activated SC accelerate melanoma growth *in vivo*

Our *in vivo* and *in vitro* human and mouse results indicate that the nerves adjacent to melanoma may be continuously undergoing degeneration/repair due to the damage of the nerve fibers by the expanding tumor and/or the direct effect of melanoma-derived factors on nerve fibers and SC. We hypothesized that tumor-associated SC activities including immune system modulation, ECM reorganization and growth factor/cytokine/chemokine production create conditions within the melanoma microenvironment favorable to tumor growth. To test if activation of SC affects melanoma growth *in vivo*, we implanted B16 cells and SC alone or together (SC + B16) orthotopically into syngeneic mice. Tumors composed of B16 cells alone grew significantly slower compared to those which contained B16 and SC (Fig. 6A). When SC were treated with minocycline *in vitro* prior to their co-injection with melanoma cells, the tumors (SC/minocycline + B16) grew at the same rate as the tumors composed of B16 cells alone, demonstrating that only functional repair-like activated SC are able to enhance tumor growth (Fig. 5A). Importantly, melanoma cells and SC do not have any direct effect on each other's proliferation rates *in vitro*, and minocycline does not affect SC viability or proliferation (Supplementary Fig. S4A–G). As expected, SC cultured in either non-conditioned medium (SC) or B16-conditioned medium (SC/B16) and injected without B16 cells did not produce tumors in mice (Fig. 6A). Our results, therefore, suggest that SC

injected with malignant cells contribute to melanoma growth by modulating the tumor microenvironment. This result raises the question whether the endogenous rSC of the skin can also promote melanoma growth.

To generate rSC in the skin, we utilized a previously described transection model of the dorsal cutaneous thoracic sensory nerves.[25] With this method the sensory nerves are cut proximal to their entrance into the skin, avoiding the injury to the denervated skin and the disruption of the vasculature and other skin components (Supplementary Fig. S5A). We confirmed utilizing C57Bl/6 mice that nerve transection leads to the upregulation of nerve injury markers in the DRG of the cut nerves (Supplementary Fig. S5B) and in SC of nerve segments distal to the cut (Supplementary Fig. S5C, D). Sensory nerve transection also resulted in the upregulation of GAP43 and $p75^{NTR}$ by neurons/SC within skin supplied by the cut nerve (Supplementary Fig. S5E–G). Furthermore, denervated and migrating SC were detectable in the skin after nerve transection (Supplementary Fig. S5H). These results confirm that selective sensory nerve transection technique induces nerve repair and generates endogenous activated rSC in the acutely denervated skin.

Utilizing both transplantable B16 and inducible BP melanoma models, we tested if selective acute transection of sensory nerves, which transforms cutaneous SC into rSC, affects subsequent melanoma growth *in vivo*. Intradermal minocycline injections were performed prior to nerve transection to block the activation of SC after nerve injury (Fig. 6B). The timing of minocycline injections was chosen to minimize any off-target effects, particularly on the tumor-infiltrating immune cells or nerve transection-associated inflammation. Transection of the sensory nerve one day before B16 cell injection significantly accelerated tumor growth compared with sham surgery or no surgery control groups (Fig. 6C). However, local injection of minocycline to inhibit SC prior to nerve transection and melanoma cell injection caused the melanoma to grow at a rate comparable to the sham surgery group (Fig. 6C), suggesting that activated rSC can facilitate melanoma growth *in vivo*. These results were confirmed with an inducible melanoma model. Nerve transection in BP mice was performed one week after melanoma induction with topical 4-HT, as previously described, [22, 25] and following minocycline injections (Fig. 6D). As with the orthotopic B16 tumors, $BRAF^{V600E}/PTEN^{null}$ driven melanoma grew faster after sensory nerve transection compared with sham or no surgery control groups, but not when the animals were locally treated with minocycline (Fig. 6E). In case of spontaneous melanoma model, off-target effects of minocycline were again minimized by locally injecting minocycline for one week before nerve transection and three weeks before first appearance of tumors. Taken together, these results indicate that SC-dependent alterations of the local microenvironment following sensory nerve injury promote tumor growth.

In summary, our results reveal that both human and mouse melanoma can reprogram SC into cells bearing strong phenotypic and functional resemblance to rSC induced by the nerve injury/Wallerian degeneration. Both melanoma-activated SC and rSC generated by nerve transection are capable of accelerating tumor growth *in vivo* in orthotopic and inducible mouse melanoma models.

DISCUSSION

It has been established in various solid tumor models that the interaction between peripheral nerves and malignant cells may accelerate cancer progression.[37] The most compelling evidence of PNS involvement in cancer comes from studies of the sympathetic nervous system.[38] β-adrenergic blockade is being tested as a treatment option for several malignancies.[39] In comparison, little attention has been directed at the peripheral neuroglia as a potential modulator of cancer.[11] Myelinating and non-myelinating SC comprise the majority of the peripheral glia and are present in almost every anatomical site in the body. To date, SC have been implicated in facilitating cancer cell neurotropism and PNI.[12] We demonstrate here that the well-known, vital functions of SC involved in orchestrating nerve and tissue repair can be activated directly by the malignant cells and can promote tumor growth *in vivo*.

Our investigation of human melanoma innervation revealed a significant reduction of intratumoral nerve fibers and SC compared to the normal skin or tissue adjacent to the tumor. This finding contrasts the reports on cancers of the prostate, stomach and pancreas, where intratumoral innervation appears to be important for tumor growth and progression.[1, 2, 4] We concluded that, unlike other solid cancers, melanoma invasion in the dermis may be destroying or displacing the nerves. This interpretation explains our finding that significantly more neural tissue related genes, particularly those which are upregulated after nerve injury, are expressed in the tissue adjacent to the melanoma while neurodegeneration processes are enriched inside the tumor. The perturbation of the intratumoral nerves by melanoma is also consistent with our observations that nerves and SC at the tumor edges phenotypically mimic those responding to neurotrauma.[10, 17, 18] Of note, most of the intratumoral nerve/SC markers we detected are known to be strongly expressed by melanoma cells.[29, 40, 41] Therefore, there appears to be a steady-state between the nerve wounding caused by the melanoma, and the perpetual attempt by the nerves surrounding the tumor to repair themselves. Such a model of constant neural repair within the tumor microenvironment is reminiscent of a well-established concept comparing a tumor to a non-healing wound.[42]

Schwann cells are at the center of the PNS regenerative process primarily because of their ability to trans-differentiate into rSC in response to nerve injury.[43] We have revealed here that SC repair-like program can be directly initiated by melanoma cells. Specifically, in a cell-cell contact-independent manner, malignant cells induce alterations in the gene expression of SC, highly resembling SC to rSC trans-differentiation after nerve injury.[10, 17, 18] We also show that these melanoma-transdifferentiated SC are functionally similar to Wallerian degeneration-associated rSC: they demonstrate enhanced motility, ECM reorganization, macrophage attraction and polarization to tissue repair M2 type.[10, 19, 20, 32] Furthermore, we found that the effect of melanoma on SC is similar between mouse and human cells, and can be blocked by minocycline, a previously described inhibitor of SC nerve repair-associated functions.[35, 36] These results support a novel paradigm in which melanoma cells reprogram SC, thereby initiating a nerve injury response in the surrounding tissue. How melanoma cells reprogram SC remains unclear. Having a common neural crest progenitor, melanoma cells share several signaling axes with the nervous system: neurotrophic factors such as nerve growth factor and glia maturation factor, ephrins,

semaphorins, neuregulins, and others. Determining melanoma-derived factors which reprogram SC is an important goal of the ongoing research.

The multitude of tasks carried out by rSC with direct consequences on the local microenvironment raises an important question of rSC influence on melanoma growth and progression. To that end, we performed a ‘gain of function’ experiment by selectively transecting dorsal cutaneous sensory nerves in transplantable and inducible mouse melanoma models. We found that melanoma grew faster during the acute response to denervation, when Wallerian degeneration and SC trans-differentiation into rSC were occurring. It is important to highlight the difference between this approach and the reported ablation of nerves in the preclinical studies of other solid cancer models. Many of those studies found that local autonomic or sensory nerve blockade decreased tumor growth.[1–4] In those cases, the methodological aim was not to induce an immediate neuronal response to injury as demonstrated here, but to block nerve signaling for a prolonged period of time. Therefore, the principal difference between our data and published reports arose because we addressed how the acute induction of SC-dependent nerve repair, not a chronic nerve inhibition, influences melanoma growth.

We determined that minocycline inhibition of nerve transection-induced or melanoma-induced activation of SC slowed melanoma growth. Minocycline also has well-described immunosuppressive properties.[44] To minimize off-target effects of minocycline, particularly on the immune cells recruited by nerve injury or melanoma, the drug was injected before nerve transection and before initiation of tumors. Thus, minocycline acted on SC before skin infiltration by the immune cells took place. Importantly, minocycline did not have any appreciable effect on tumor growth in sham-surgery groups of either transplantable or inducible melanoma model, demonstrating that its direct effect on macrophages and other immune cells in our model is negligible. Therefore, primary effect of minocycline in our models is the inhibition of nerve injury-induced SC activation, consistent with previous reports.[35, 36]

As we found no direct effect of SC on melanoma cell proliferation, we conclude that the accelerated tumor growth *in vivo* observed in all tested melanoma models is due to the modulation of the local microenvironment by activated SC. This interpretation is consistent with well-established and emerging effects of rSC on the surrounding tissue.[10–12, 19, 20] To our knowledge, our results are the first to demonstrate that repair-like SC activity may be triggered by melanoma cells directly, and may promote tumor growth and progression.

While we demonstrated that neurodegenerative reprogramming of SC can promote malignant growth, we have not addressed the potential involvement of neuronal axons in this process. Axons and SC exist in a constant state of interaction, which is especially important during nerve injury and regeneration.[10, 17, 18] We have observed that DRG of the neurons located within the melanoma-harboring dermatome express markers of nerve injury.[33, 34] In addition, we have previously shown, using an orthotopic melanoma model, that DRG neurons may promote tumor growth *in vivo*.[45] Therefore, it is likely that both SC and axons participate in the nerve repair response triggered by melanoma. Elucidating the

mechanism of the interaction among malignant cells, axons and SC is critically important to our understanding of the forces which help create a tumor-permissive microenvironment.

Our results raise new important questions of how nerve injury is instigated in and around the tumor, and to what extent it influences the initiation, survival, growth and invasion of various types of cancer. Additionally, how do regenerative growth of injured nerves and collateral sprouting contribute to the conditions favorable for tumor growth? Our data suggest that there likely are several tumor-promoting rSC activities working in parallel, including local immunosuppression and ECM breakdown. Furthermore, we and others have shown that SC, especially trans-differentiated SC, strongly attract and increase the motility of malignant cells.[15, 46] Together, these SC functions within primary tumor or distal organs may significantly increase melanoma's metastatic potential, similarly to what we have demonstrated with lung carcinoma cells.[46]

Targeting tumor-associated neuronal tissue is an emerging strategy for cancer treatment. Current clinical trial efforts in this field, however, are limited to the inhibition of synaptic or post-synaptic signaling, primarily of the beta-adrenergic system. Our results demonstrate that the neuronal repair process within the tumor microenvironment may be an important contributor to cancer progression, and therefore, represents a novel target for cancer therapy. Developing SC-specific inhibitors to disrupt the cancer-nerve/SC-immune system axis offers a new and promising therapeutic approach.

Supplementary Material

Refer to Web version on PubMed Central for supplementary material.

Acknowledgments:

This work was funded in part by UPCI Melanoma and SPORE in Skin Cancer Career Enhancement Program Award P50CA121973 (YLB), Skin Cancer Foundation Research Grant (YLB), London Foundation Grant LAGBL-0271–2013 (MRS), R21CA191522 (ZY), RO1CA196286 (AEL). This project used UPCI Cancer Biomarkers, Genomics and Biostatistics Facilities which are supported in part by award P30CA047904 and the University of Pittsburgh Imaging Core that is supported in part by award P01HL114453. We thank Dr. Brian M. Davis and Dr. Jami Saloman for their technical assistance and discussions. We also thank C. Donahue Carey, D. Prosser, C. Sciulli and P. Petrosko for their technical expertise and support.

REFERENCES

1. Magnon C, Hall SJ, Lin J, Xue X, Gerber L, Freedland SJ, et al. Autonomic nerve development contributes to prostate cancer progression. Science 2013;341:1236361. [PubMed: 23846904]
2. Zhao CM, Hayakawa Y, Kodama Y, Muthupalani S, Westphalen CB, Andersen GT, et al. Denervation suppresses gastric tumorigenesis. Sci Transl Med 2014;6:250ra115.
3. Peterson SC, Eberl M, Vagnozzi AN, Belkadi A, Veniaminova NA, Verhaegen ME, et al. Basal cell carcinoma preferentially arises from stem cells within hair follicle and mechanosensory niches. Cell Stem Cell 2015;16:400–12. [PubMed: 25842978]
4. Saloman JL, Albers KM, Li D, Hartman DJ, Crawford HC, Muha EA, et al. Ablation of sensory neurons in a genetic model of pancreatic ductal adenocarcinoma slows initiation and progression of cancer. Proc Natl Acad Sci U S A 2016;113:3078–83. [PubMed: 26929329]
5. Schmidt BL, Hamamoto DT, Simone DA, Wilcox GL. Mechanism of cancer pain. Mol Interv 2010;10:164–78. [PubMed: 20539035]

6. Selvaraj D, Kuner R. Molecular players of tumor-nerve interactions. Pain 2015;156:6–7. [PubMed: 25599295]
7. Ceyhan GO, Demir IE, Altintas B, Rauch U, Thiel G, Muller MW, et al. Neural invasion in pancreatic cancer: a mutual tropism between neurons and cancer cells. Biochem Biophys Res Commun 2008;374:442–7. [PubMed: 18640096]
8. Pavri SN, Clune J, Ariyan S, Narayan D. Malignant Melanoma: Beyond the Basics. Plast Reconstr Surg 2016;138:330e–40e.
9. Mahar AL, Compton C, Halabi S, Hess KR, Gershenwald JE, Scolyer RA, et al. Critical Assessment of Clinical Prognostic Tools in Melanoma. Ann Surg Oncol 2016;23:2753–61. [PubMed: 27052645]
10. Jessen KR, Mirsky R. The repair Schwann cell and its function in regenerating nerves. J Physiol 2016;594:3521–31. [PubMed: 26864683]
11. Bunimovich YL, Keskinov AA, Shurin GV, Shurin MR. Schwann cells: a new player in the tumor microenvironment. Cancer Immunol Immunother 2017;66:959–68. [PubMed: 27885383]
12. Deborde S, Wong RJ. How Schwann cells facilitate cancer progression in nerves. Cell Mol Life Sci 2017;74:4405–20. [PubMed: 28631007]
13. Kidd GJ, Ohno N, Trapp BD. Biology of Schwann cells. Handb Clin Neurol 2013;115:55–79. [PubMed: 23931775]
14. Griffin JW, Thompson WJ. Biology and pathology of nonmyelinating Schwann cells. Glia 2008;56:1518–31. [PubMed: 18803315]
15. Deborde S, Omelchenko T, Lyubchik A, Zhou Y, He S, McNamara WF, et al. Schwann cells induce cancer cell dispersion and invasion. J Clin Invest 2016;126:1538–54. [PubMed: 26999607]
16. Mika J, Zychowska M, Popiolek-Barczyk K, Rojewska E, Przewlocka B. Importance of glial activation in neuropathic pain. Eur J Pharmacol 2013;716:106–19. [PubMed: 23500198]
17. Glenn TD, Talbot WS. Signals regulating myelination in peripheral nerves and the Schwann cell response to injury. Curr Opin Neurobiol 2013;23:1041–8. [PubMed: 23896313]
18. Boerboom A, Dion V, Chariot A, Franzen R. Molecular Mechanisms Involved in Schwann Cell Plasticity. Front Mol Neurosci 2017;10:38. [PubMed: 28261057]
19. Parfejevs V, Debbache J, Shakhova O, Schaefer SM, Glausch M, Wegner M, et al. Injury-activated glial cells promote wound healing of the adult skin in mice. Nat Commun 2018;9:236. [PubMed: 29339718]
20. Clements MP, Byrne E, Camarillo Guerrero LF, Cattin AL, Zakka L, Ashraf A, et al. The Wound Microenvironment Reprograms Schwann Cells to Invasive Mesenchymal-like Cells to Drive Peripheral Nerve Regeneration. Neuron 2017;96:98–114 e7. [PubMed: 28957681]
21. Dankort D, Curley DP, Cartlidge RA, Nelson B, Karnezis AN, Damsky WE Jr., et al. Braf(V600E) cooperates with Pten loss to induce metastatic melanoma. Nat Genet 2009;41:544–52. [PubMed: 19282848]
22. Zhang Y, Chen G, Liu Z, Tian S, Zhang J, Carey CD, et al. Genetic vaccines to potentiate the effective CD103+ dendritic cell-mediated cross-priming of antitumor immunity. J Immunol 2015;194:5937–47. [PubMed: 25972487]
23. Cooper ZA, Juneja VR, Sage PT, Frederick DT, Piris A, Mitra D, et al. Response to BRAF inhibition in melanoma is enhanced when combined with immune checkpoint blockade. Cancer Immunol Res 2014;2:643–54. [PubMed: 24903021]
24. Aznavoorian S, Moore BA, Alexander-Lister LD, Hallit SL, Windsor LJ, Engler JA. Membrane type I-matrix metalloproteinase-mediated degradation of type I collagen by oral squamous cell carcinoma cells. Cancer Res 2001;61:6264–75. [PubMed: 11507081]
25. Siebenhaar F, Magerl M, Peters EM, Hendrix S, Metz M, Maurer M. Mast cell-driven skin inflammation is impaired in the absence of sensory nerves. J Allergy Clin Immunol 2008;121:955–61. [PubMed: 18158175]
26. Laverdet B, Danigo A, Girard D, Magy L, Demiot C, Desmouliere A. Skin innervation: important roles during normal and pathological cutaneous repair. Histol Histopathol 2015;30:875–92. [PubMed: 25799052]
27. Yi S, Tang X, Yu J, Liu J, Ding F, Gu X. Microarray and qPCR Analyses of Wallerian Degeneration in Rat Sciatic Nerves. Front Cell Neurosci 2017;11:22. [PubMed: 28239339]

28. Shin JE, Ha H, Cho EH, Kim YK, Cho Y. Comparative analysis of the transcriptome of injured nerve segments reveals spatiotemporal responses to neural damage in mice. J Comp Neurol 2018;526:1195–208. [PubMed: 29405296]
29. Uhlen M, Fagerberg L, Hallstrom BM, Lindskog C, Oksvold P, Mardinoglu A, et al. Proteomics. Tissue-based map of the human proteome. Science 2015;347:1260419. [PubMed: 25613900]
30. Napoli I, Noon LA, Ribeiro S, Kerai AP, Parrinello S, Rosenberg LH, et al. A central role for the ERK-signaling pathway in controlling Schwann cell plasticity and peripheral nerve regeneration in vivo. Neuron 2012;73:729–42. [PubMed: 22365547]
31. Tofaris GK, Patterson PH, Jessen KR, Mirsky R. Denervated Schwann cells attract macrophages by secretion of leukemia inhibitory factor (LIF) and monocyte chemoattractant protein-1 in a process regulated by interleukin-6 and LIF. J Neurosci 2002;22:6696–703. [PubMed: 12151548]
32. Stratton JA, Shah PT. Macrophage polarization in nerve injury: do Schwann cells play a role? Neural Regen Res 2016;11:53–7. [PubMed: 26981078]
33. Linda H, Skold MK, Ochsmann T. Activating transcription factor 3, a useful marker for regenerative response after nerve root injury. Front Neurol 2011;2:30. [PubMed: 21629765]
34. Tsujino H, Kondo E, Fukuoka T, Dai Y, Tokunaga A, Miki K, et al. Activating transcription factor 3 (ATF3) induction by axotomy in sensory and motoneurons: A novel neuronal marker of nerve injury. Mol Cell Neurosci 2000;15:170–82. [PubMed: 10673325]
35. Keilhoff G, Langnaese K, Wolf G, Fansa H. Inhibiting effect of minocycline on the regeneration of peripheral nerves. Dev Neurobiol 2007;67:1382–95. [PubMed: 17638380]
36. Pinkernelle J, Fansa H, Ebmeyer U, Keilhoff G. Prolonged minocycline treatment impairs motor neuronal survival and glial function in organotypic rat spinal cord cultures. PLoS One 2013;8:e73422. [PubMed: 23967343]
37. Saloman JL, Albers KM, Rhim AD, Davis BM. Can Stopping Nerves, Stop Cancer? Trends Neurosci 2016;39:880–89. [PubMed: 27832915]
38. Cole SW, Nagaraja AS, Lutgendorf SK, Green PA, Sood AK. Sympathetic nervous system regulation of the tumour microenvironment. Nat Rev Cancer 2015;15:563–72. [PubMed: 26299593]
39. Braadland PR, Ramberg H, Grytli HH, Tasken KA. beta-Adrenergic Receptor Signaling in Prostate Cancer. Front Oncol 2014;4:375. [PubMed: 25629002]
40. Slutsky SG, Kamaraju AK, Levy AM, Chebath J, Revel M. Activation of myelin genes during transdifferentiation from melanoma to glial cell phenotype. J Biol Chem 2003;278:8960–8. [PubMed: 12643284]
41. Luo C, Pietruska JR, Sheng J, Bronson RT, Hu MG, Cui R, et al. Expression of oncogenic BRAFV600E in melanocytes induces Schwannian differentiation in vivo. Pigment Cell Melanoma Res 2015;28:603–6. [PubMed: 26036358]
42. Dvorak HF. Tumors: wounds that do not heal. Similarities between tumor stroma generation and wound healing. N Engl J Med 1986;315:1650–9. [PubMed: 3537791]
43. Jessen KR, Mirsky R, Lloyd AC. Schwann Cells: Development and Role in Nerve Repair. Cold Spring Harb Perspect Biol 2015;7:a020487. [PubMed: 25957303]
44. Garrido-Mesa N, Zarzuelo A, Galvez J. Minocycline: far beyond an antibiotic. Br J Pharmacol 2013;169:337–52. [PubMed: 23441623]
45. Keskinov AA, Tapias V, Watkins SC, Ma Y, Shurin MR, Shurin GV. Impact of the Sensory Neurons on Melanoma Growth In Vivo. PLoS One 2016;11:e0156095. [PubMed: 27227315]
46. Zhou Y, Shurin GV, Zhong H, Bunimovich YL, Han B, Shurin MR. Schwann cells augment cell spreading and metastasis of lung cancer. Cancer Res 2018;78:5927–39. [PubMed: 30135194]

Significance

Findings reveal a role of the nerve injury response, particularly through functions of activated Schwann cells, in promoting melanoma growth.

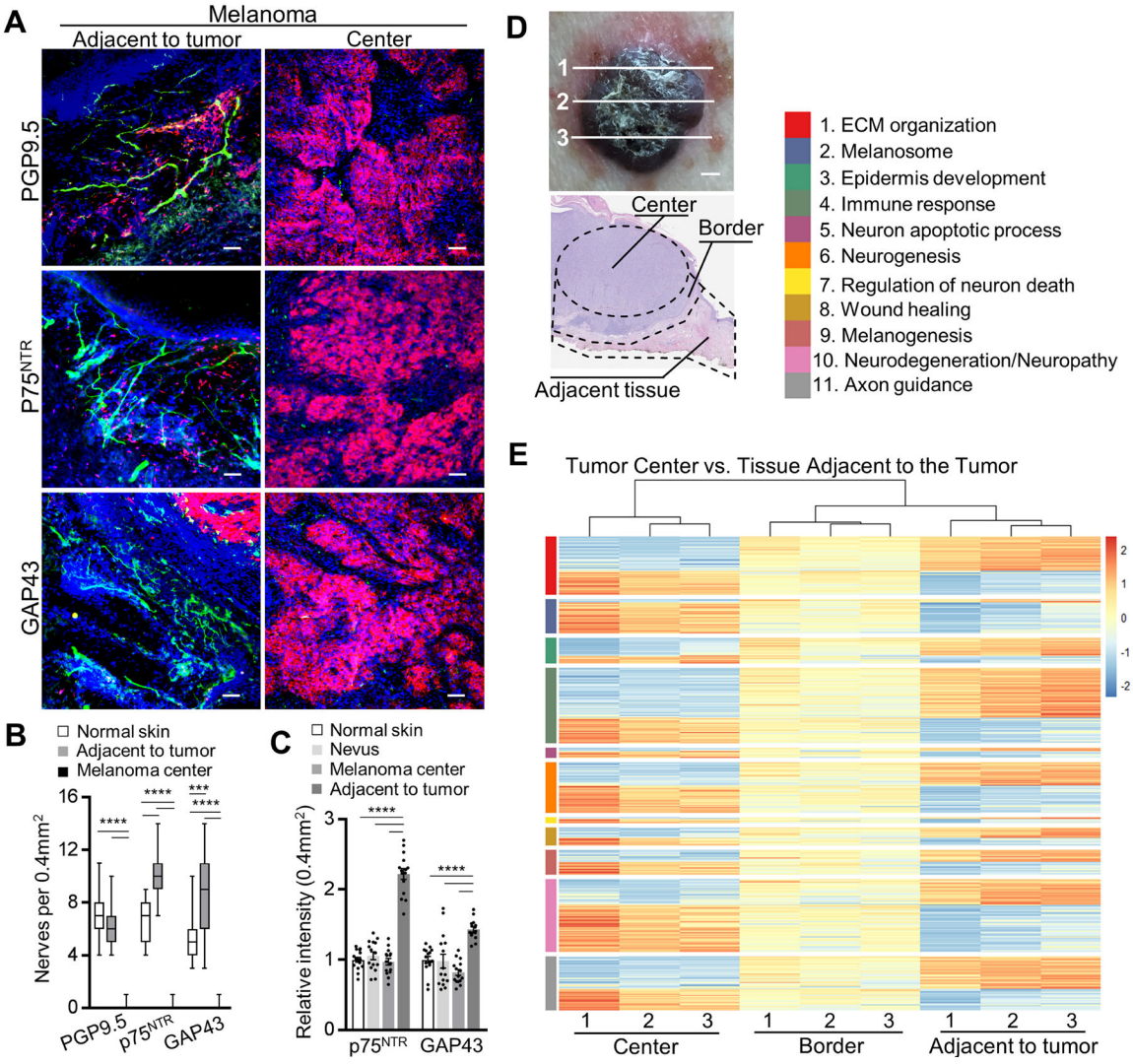

Figure 1. Phenotypic and functional dysregulation of nerve fibers in human melanoma.

(**A**) Representative immunofluorescence images of nerves (green: PGP9.5 – nerve fiber, $p75^{NTR}$ – SC, GAP43 – nerves/SC; red: MITF – melanoma; blue: DAPI) in the **center** of primary cutaneous human melanoma or the tissue **adjacent to the tumor**. Scale bars: 50 μm. (**B**) Enumeration of neuronal projections in 0.4 mm^2 of normal human skin, in the center of human primary cutaneous melanoma or in the tissue adjacent to the tumor using immunostaining for nerve fiber and SC markers PGP9.5, $p75^{NTR}$, GAP43. Center line, median; box limits, upper and lower quartiles; whiskers, max and min. (**C**) Relative fluorescence intensities of $p75^{NTR}$ and GAP43 immunostained normal human skin, human nevi and melanoma. Image intensities (average over 0.4 mm^2 visual field) were normalized to normal skin average. (**D**) Top panel: optical image of human melanoma sectioned at three different areas (labeled 1, 2, 3). Bottom panel: H&E image showing three domains – tumor center (labeled *Center*), tumor edge (labeled *Border*), stroma adjacent to the tumor (labeled *Adjacent tissue*), micro-dissected and used for RNA-sequencing. (**E**) Heat map of NIH DAVID pathway enrichment analysis using differentially expressed genes with $p < 0.05$

from pairwise comparison between melanoma tumor center and the tissue adjacent to the tumor. Data are means ± SEM; n = 3 independent samples with five different 0.4 mm^2 images per sample, one-way ANOVA with Tukey's multiple comparisons test (B, C). *P<0.05, **P<0.01, ***P<0.001, ****P<0.0001.

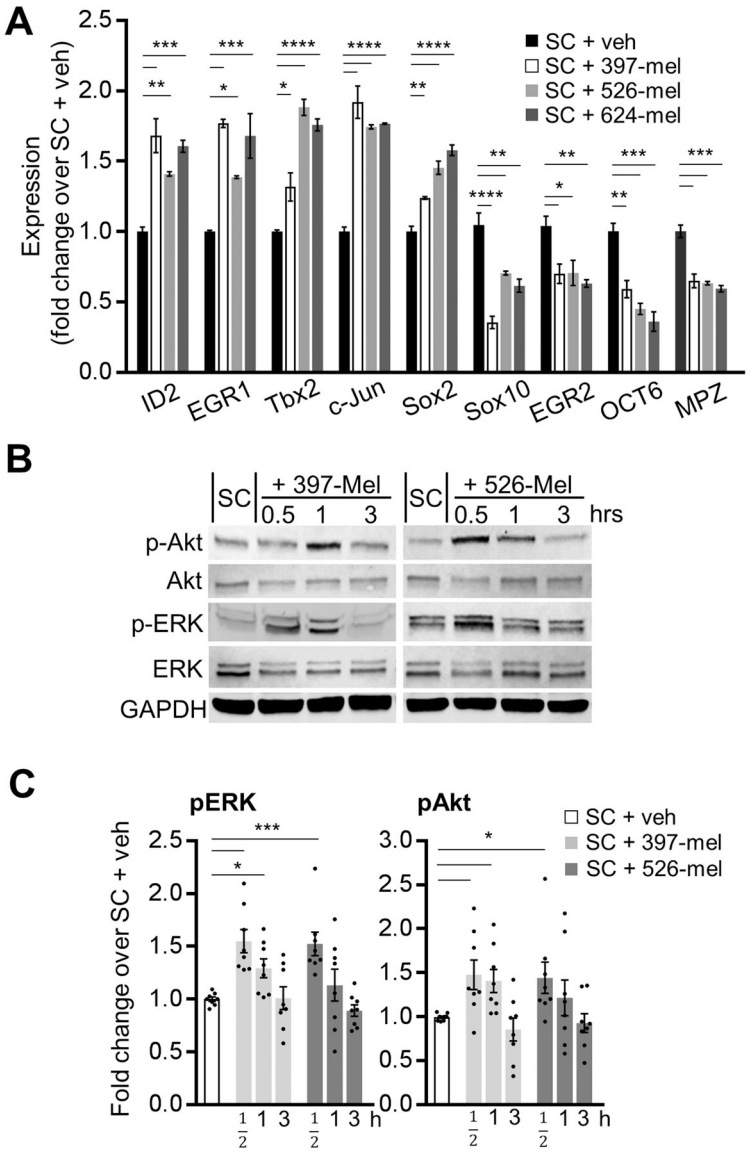

Figure 2. Human melanoma cells induce phenotypic changes in Schwann cells characteristic of degenerating nerves.

(**A**) Transcript levels of mature and activated rSC genetic markers in SC cultures treated for 48 h with 20% (v/v) of either non-conditioned medium (RPMI-1640, veh) or conditioned medium from 397-mel, 526-mel or 624-mel cell lines. Transcript levels were determined by qRT-PCR and were normalized to those in vehicle-treated SC; n = 3. (**B**) Representative Western blots for total and p-Erk1/2 (Thr202/Tyr204) and p-Akt (Ser473) in cultured human SC at 30 min, 1 h and 3 h after treatment with 20% (v/v) of either non-conditioned medium (RPMI-1640, veh) or conditioned medium from 397-mel or 526-mel cell lines. GAPDH was used as a housekeeping control. (**C**) Densitometry analysis of the Western blots as shown in (B). Phosphorylated proteins were normalized to total protein levels; n = 8. Data are means ± SEM; one-way ANOVA with Tukey's multiple comparisons test (A, C). *P<0.05, **P<0.01, ***P<0.001, ****P<0.0001.

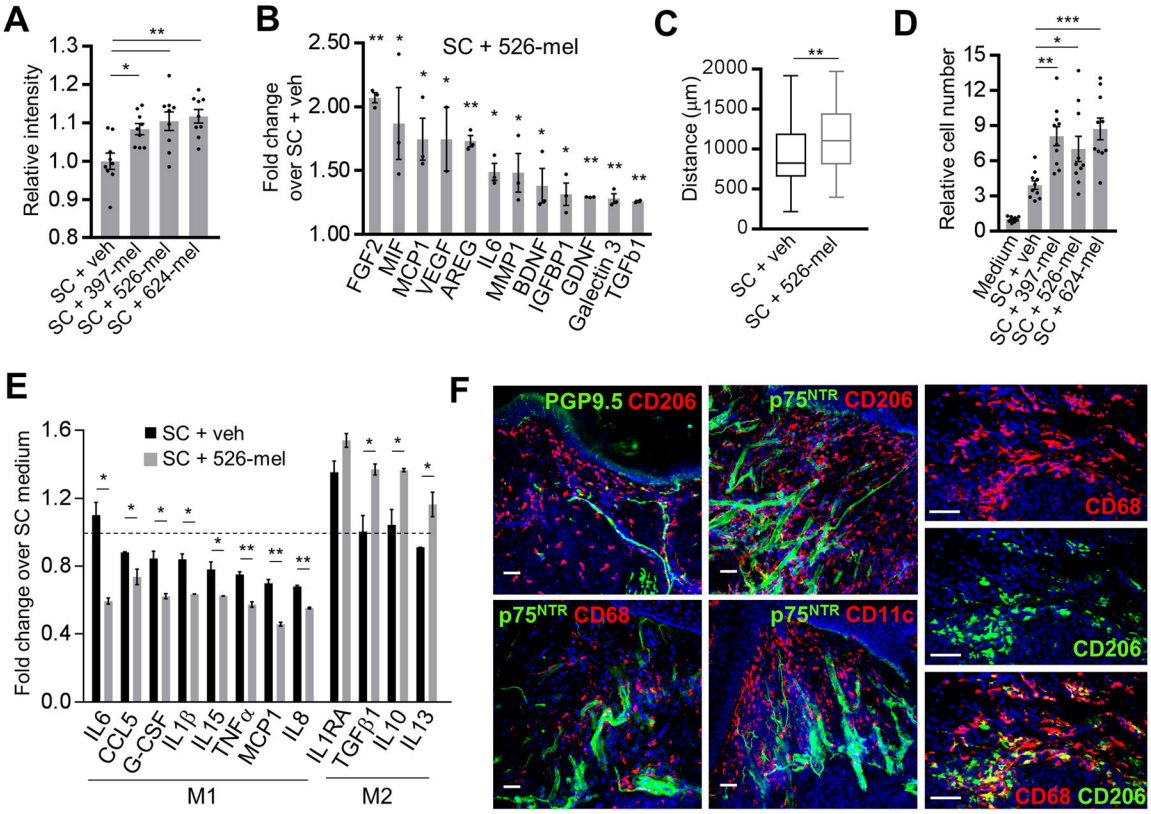

Figure 3. Human melanoma cells induce functional changes in Schwann cells characteristic of degenerating nerves.

(**A**) Collagen I breakdown by SC cultured for 96 h in 20% (v/v) of either RPMI-1640 (veh) or conditioned medium from 397-mel, 526-mel or 624-mel cell lines. Data are presented as relative intensity of light transmitted through the collagen film; n = 9. (**B**) Luminex multiplex assay showing protein concentrations in supernatants of human SC cultures treated for 48 h with 20% (v/v) 526-mel conditioned medium. Data are presented relative to protein concentrations in supernatants of human SC cultures treated with 20% (v/v) RPMI-1640 (veh). Supernatant was collected from washed SC over 48 h. Protein levels (in pg/ml) were normalized to cell density in cultures. Medium was used as a background control; n = 3. (**C**) Migration assay of SC (10^5 cells) plated within ECM gel and cultured in 20% (v/v) of either RPMI-1640 (veh) or 526-mel conditioned medium. Data are presented as distance SC migrated away from the gel edge in 56 h; n = 3, with 26 measurements per experiment at random locations around the circumference. Center line, median; box limits, upper and lower quartiles; whiskers, max and min. (**D**) Transwell Matrigel migration of THP-1 derived macrophages (top chamber) toward bottom chamber containing 20% (v/v) of either SC medium or supernatant from SC pretreated for 48 h with 20% (v/v) of: non-conditioned medium (veh) or melanoma-conditioned (397-mel, 526-mel, 624-mel) medium. Macrophages on the membrane after 48 h were stained with hematoxylin and counted; n = 10. (**E**) Luminex multiplex assay showing cytokine concentrations in supernatants of THP-1 derived macrophage cultures treated for 48 h with 20% (v/v): (i) SC medium, (ii) supernatants from SC cultures pretreated with 20% (v/v) RPMI-1640 (veh), or (iii) supernatants from SC cultures pretreated with 20% (v/v) 526-mel conditioned medium.

Supernatant was collected from washed SC over 48 h and used in macrophage cultures. Cytokine concentrations (in pg/ml) were normalized to cell densities in cultures. Medium was used as a background control. Data were normalized to SC medium only (represented by dashed line); n = 3. Cytokines are grouped by their association with either M1 or M2 macrophage subtype. (**F**) Left and middle columns: representative immunofluorescence images of the neurons (green: PGP9.5 – nerve fiber, $p75^{NTR}$– SC) colocalizing with macrophages (red: CD68, CD206) and dendritic cells (red: CD11c) in the tissue adjacent to primary human melanoma. Right column: co-labelled M2 macrophages ($CD68^{+}/CD206^{+}$) in the tissue adjacent to melanoma. Blue: DAPI. Scale bars: 50 μm. Data are means ± SEM; one-way ANOVA with Tukey's multiple comparisons test (A, D), two-tailed unpaired Student's t-test (B, C, E). *P<0.05, **P<0.01, ***P<0.001, ****P<0.0001.

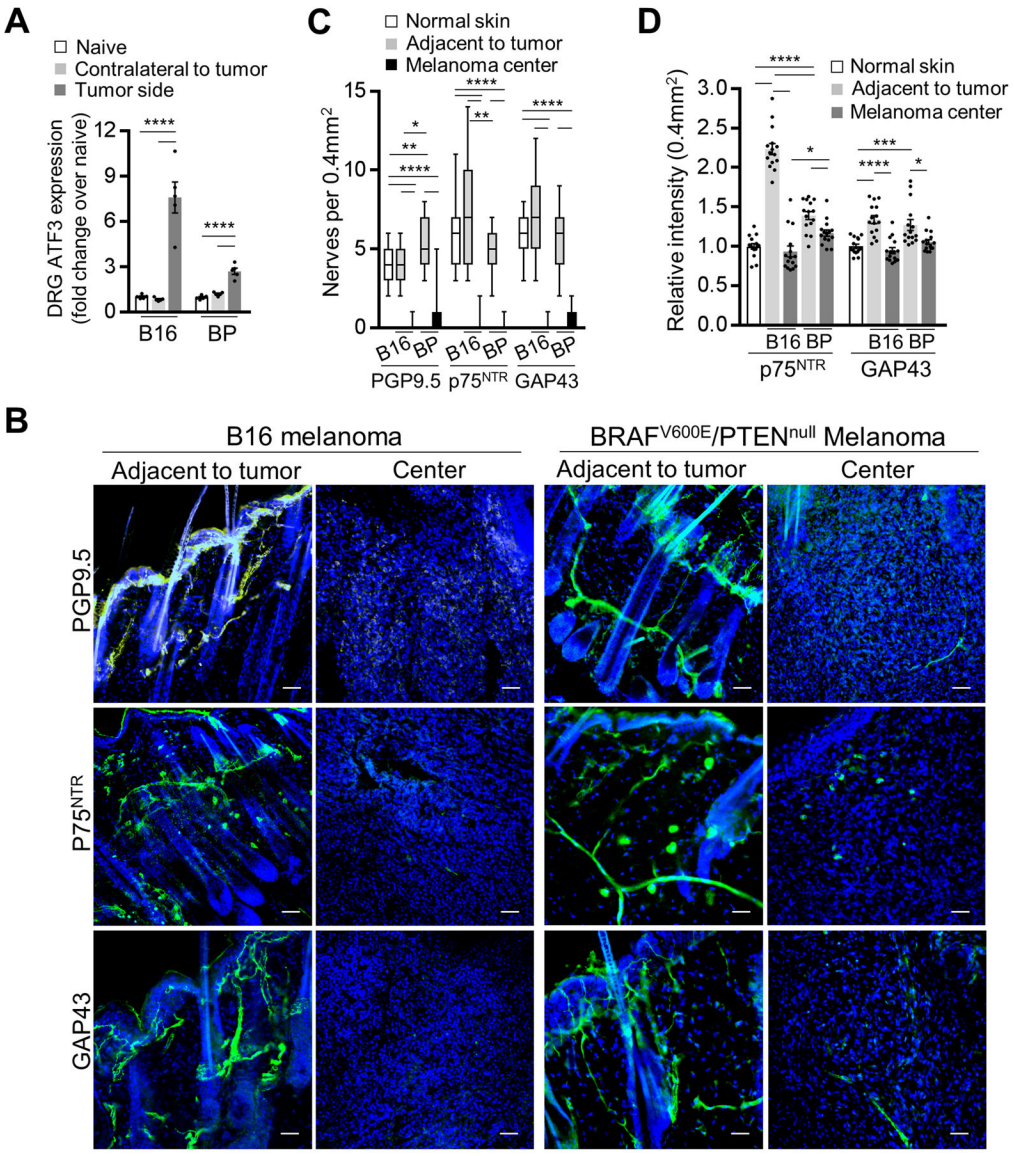

Figure 4. Mouse melanoma tumor models induce nerve injury phenotype in the adjacent nerves and Schwann cells.

(**A**) Transcript levels of ATF3 from DRG (combined T10-L2 per mouse) which supplied mouse dermatomes bearing either injected B16 cells (analyzed 2 weeks after injection) or induced BP melanoma (analyzed 2 weeks after induction). DRG from non-tumor bearing mice (labelled as *naive*) and those contralateral to the tumor served as controls. Transcript levels were determined by qRT-PCR and were normalized to those from non-tumor bearing mice; n = 5. (**B**) Representative immunofluorescence images of the nerves (green: PGP9.5 – nerve fiber, $p75^{NTR}$– SC, GAP43 – nerves/SC; blue: DAPI) in the tissue adjacent to or in the center of either implanted B16 or induced BP melanoma. Scale bars: 50 μm. (**C**) Enumeration of nerve projections detected in 0.4 mm^2 of normal mouse skin, in the center of the implanted B16 or induced BP melanoma or in the tissue adjacent to melanoma using immunostaining for nerve fiber and SC markers PGP9.5, GAP43, $p75^{NTR}$. Center line, median; box limits, upper and lower quartiles; whiskers, max and min. (**D**) Relative

fluorescence intensities of $p75^{NTR}$ and GAP43-immunostained normal mouse skin, implanted B16 and induced BP melanomas. Intensities (average over 0.4 mm^2 visual field) were normalized to normal skin average. Data are means ± SEM; n = 3 independent samples with five different 0.4 mm^2 images per sample. One-way ANOVA with Tukey's multiple comparisons test (A, C, D). *P<0.05, **P<0.01, ***P<0.001, ****P<0.0001.

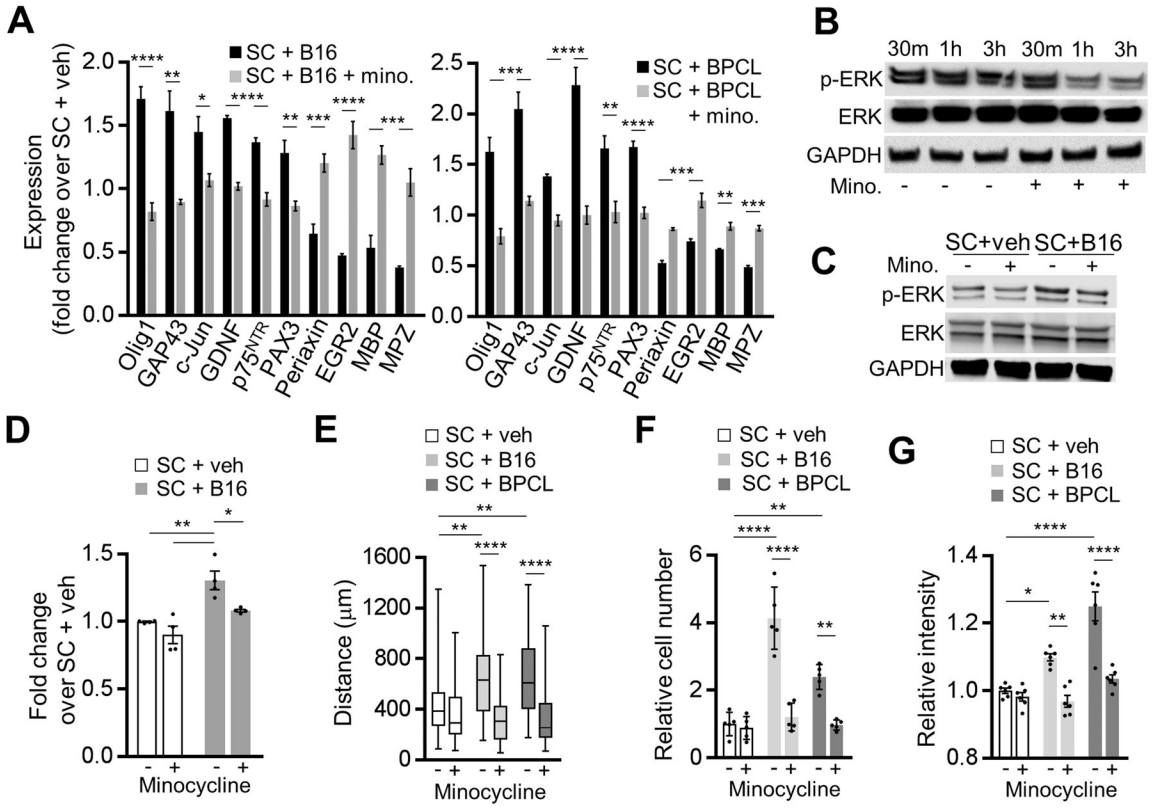

Figure 5. Murine melanoma cells facilitate Schwann cell conversion into repair-like Schwann cell.

(**A**) Transcript levels of mature and repair SC genetic markers in murine SC cultures treated for 48 h with 20% (v/v) of B16 or BPCL-conditioned medium, with or without 40 μM minocycline. Transcript levels were determined by qRT-PCR and were normalized to those of SC treated with 20% (v/v) of non-conditioned medium (veh). GAPDH was used as a housekeeping control; n = 3. (**B**) Representative Western blots for p-Erk1/2 (Thr202/Tyr204) of sciatic nerve 30 min, 1 h and 3 h after dissection from C57Bl/6 mice. Whole nerves were kept in SC medium with or without 40 μM minocycline; n = 2. (**C**) Representative Western blots for total and p-Erk1/2 (Thr202/Tyr204) in cultured murine SC 3 h after treatment with 20% (v/v) of either non-conditioned (veh) or B16-conditioned medium, with or without 40 μM minocycline. (**D**) Densitometry analysis of the Western blots as shown in (C). Phosphorylated proteins were normalized to total protein levels; n = 4. (**E**) Migration assay of murine SC plated within ECM gel (10^5 cells) and cultured in 20% (v/v) of: DMEM (veh), B16-conditioned medium, or BPCL-conditioned medium. Data are presented as distance SC migrated away from the gel edge in 56 h; n = 3, with 26 measurements per experiment at random locations around the circumference. Center line, median; box limits, upper and lower quartiles; whiskers, max and min. (**F**) Transwell Matrigel migration of RAW264.7 macrophages (top chamber) toward bottom chamber containing 20% (v/v) supernatant from murine SC pretreated for 48 h with 20% (v/v) of: DMEM (veh), B16-conditioned medium, or BPCL-conditioned medium, with or without 40 μM minocycline. Macrophages on the membrane after 48 h were stained with hematoxylin and counted; n = 5. (**G**) Collagen I breakdown by SC cultured for 7 days in 20% (v/v) of either DMEM (veh) or melanoma

(B16 or BPCL) conditioned medium, with or without 40 μM minocycline. Data are presented as relative intensity of light transmitted through the collagen film; n = 6. Data are means ± SEM; two-way ANOVA (D, E, F, G) with Tukey's multiple comparisons test; two-tailed unpaired Student's t-test (A). *P<0.05, **P<0.01, ***P<0.001, ****P<0.0001.

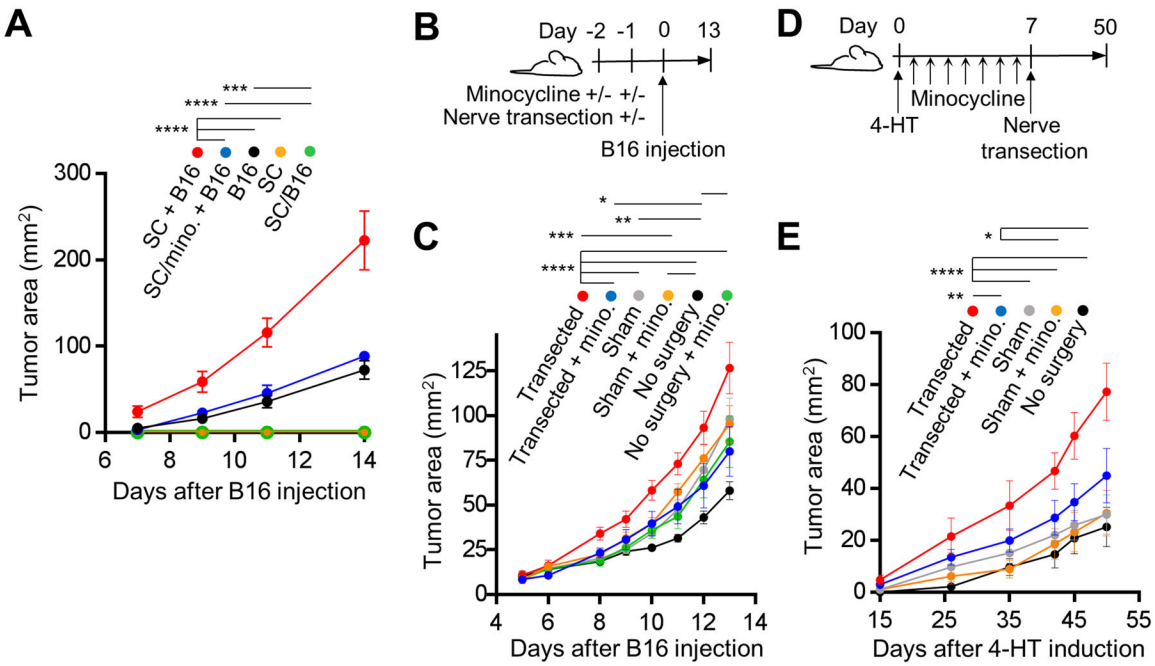

Figure 6. Activated Schwann cells stimulate melanoma growth.

(**A**) Growth curves of orthotopic B16 tumors in C57BL/6 mice: (i) B16 cells with SC (co-injected 10^5 cells of each/100 μl), labeled *SC + B16*, (ii) B16 cells co-injected with SC which were first pretreated for 48 h in culture with 40 μM minocycline and washed, labeled *SC/mino+B16*, (iii) B16 cells alone (10^5 cells/100 μl injected), labeled *B16*, (iv) SC alone (10^5 cells/100 μl), labeled *SC*, (v) SC alone (10^5 cells/100 μl) pretreated for 48 h in culture with 20% (v/v) B16-conditioned medium prior to injection, labeled *SC/B16*; n = 2 independent experiments, 5 mice per group per experiment. (**B**) Timeline of the dorsal cutaneous sensory nerve transection experiment with C57BL/6 mice and orthotopic B16 melanoma model. Minocycline (10 μM) was injected twice on day −2 and once on day −1 in the site of B16 injection on day 0. Nerve transection or sham surgery was performed one day before the B16 injection. (**C**) Growth rates of B16 melanoma in C57BL/6 mice treated as described in (B). Nerves were either transected or mice underwent sham surgery or no surgery; n = 2 independent experiments with 8 mice per group. (**D**) Timeline of the dorsal cutaneous sensory nerve transection experiment with inducible $Braf^{V600E}$/$PTEN^{null}$ melanoma model. On day 0, tumors were induced with topical application of 4-HT on lateral back at T8–T11 dermatomes. For minocycline treatment groups, the drug was injected intradermally (10 μM) daily at the site of 4-HT application for 7 days. Nerve transection or sham surgeries were performed one week after tumor induction. (**E**) Growth rates of BP melanoma in mice treated as described in (D). Nerves were either transected or mice underwent sham surgery; n = 2 independent experiments with 8 mice per group. Data are means ± SEM; two-way ANOVA with Tukey's multiple comparisons test (A, C, E). *P<0.05, **P<0.01, ***P<0.001, ****P<0.0001.